

NTIS HC \$4.25

X-651-72-458

PREPRINT

NASA TM X- 66143

# SPACE OBSERVATIONS OF THE VARIABILITY OF SOLAR IRRADIANCE IN THE NEAR AND FAR ULTRAVIOLET

DONALD F. HEATH

(NASA-TM-X-66143) SPACE OBSERVATIONS OF  
THE VARIABILITY OF SOLAR IRRADIANCE IN  
THE NEAR AND FAR ULTRAVIOLET (NASA)  
45 p HC \$4.25

N73-16794

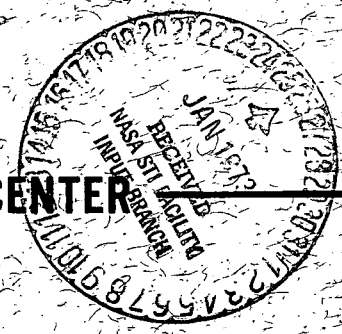
CSCL 03B

G3/29

Unclas  
52963



GODDARD SPACE FLIGHT CENTER  
GREENBELT, MARYLAND



SPACE OBSERVATIONS OF THE VARIABILITY  
OF SOLAR IRRADIANCE IN THE NEAR AND FAR ULTRAVIOLET

Donald F. Heath  
Goddard Space Flight Center  
Greenbelt, Maryland 20771

**Preceding page blank**

SPACE OBSERVATIONS OF THE VARIABILITY  
OF SOLAR IRRADIANCE IN THE NEAR AND FAR ULTRAVIOLET

Donald F. Heath

Goddard Space Flight Center

Greenbelt, Maryland 20771

ABSTRACT

Satellite observations of the ultraviolet solar irradiance in selected wavelength bands between 1200 and 3000Å have been made continuously by photometers consisting of broad-band sensors operated on Nimbus 3 and 4 which were launched in April, 1969 and 1970. In addition spectrophotometer measurements of the solar irradiance have been made with a dispersive instrument at 12 selected wavelengths from 2550 to 3400Å with a 10Å bandpass on Nimbus 4. Variations of the solar irradiance associated with the solar rotational period have been observed since the launch of Nimbus 3. These variations are apparently associated with two source regions separated by about 180° in solar longitude. The change in irradiance with solar rotation was found to increase with decreasing wavelengths. Different types of the observed variations in uv solar irradiance can be classified in accordance with characteristic times, e.g. in the order of increasing periods as follows: (1) Flare associated enhancements; (2) 27-day variations due to solar rotation; (3) a possible biennial effect; (4) long term variations associated with the 11-year solar cycle.

PRECEDING PAGE BLANK NOT FILMED

# Preceding page blank

## CONTENTS

	<u>Page</u>
INTRODUCTION .....	1
INSTRUMENT .....	3
RATIOMETRIC CALIBRATION .....	5
OBSERVATIONS .....	7
Absolute UV Solar Irradiance and the Solar Cycle .....	7
Variability of UV Irradiance with Solar Rotation .....	12
A Possible 22 Month Solar Variability .....	17
Flare-Related Variations of UV Irradiance .....	17
DISCUSSION .....	19
ACKNOWLEDGEMENTS .....	20
REFERENCES .....	21

PRECEDING PAGE BLANK NOT FILMED

## TABLES

<u>Table</u>	<u>Page</u>
1     Stability of the Constant Current Calibration Sources Measured with the MUSE Electrometer on Nimbus 3 (Nominal 5000 Orbits/yr.) .....	24
2     Ratio of Calculated to Observed Signals .....	25
3     Solar Irradiance Measured with a 10A Bandpass and Triangular Slit Function .....	26
4     Equivalent Solar Blackbody Temperatures .....	27
5     Correlation Coefficients of UV Solar Irradiance Maxima from Sensor A with Maxima of some Conventional Indicators of Solar Activity .....	28

## ILLUSTRATIONS

<u>Figure</u>		<u>Page</u>
1	Product of filter transmittance and photocathode quantum efficiency. The left ordinate is for sensors A and B while the right one is for C .....	29
2	Sensor response distribution is the fractional part of the total signal coming from wavelengths less than  The letters A-E refer to the sensors listed in Table 2.  The sensitivity curves (product of filter transmittance and photocathode quantum efficiency for sensors A-C) are shown in Figure 1 .....	30
3	Comparison of solar irradiance observed from Nimbus 4 with Thekaekara (1970), Labs and Neckel (1968, 1970), Makarova and Kharitonov (1969), and Tousey (1963) .....	31
4	The MUSE sensor signal currents with the exponential degradation factors removed are given to illustrate the nature of variations in irradiance associated with the 27-day solar rotational period. Other indicators of solar activity are given for the same period .....	32
5	Percentage uv variation per solar rotation ( $I_{\max}-I_{\min}/I_{\min}$ ) with the wavenumber of the 0.5 point in Figure 2 observed with the three sensors on Nimbus 3 near solar maximum .....	33

## ILLUSTRATIONS (continued)

<u>Figure</u>		<u>Page</u>
6	Carrington longitude of the central meridian on the days of observed uv maxima in irradiance. The different symbols represent different regions on the basis of groupings in longitude .....	34
7	Observations of the percentage variation per solar rotation observed with sensor A on Nimbus 3 and 4 .....	35
8	Overlap in time of the sensor A signals observed from Nimbus 3 and 4 for the period beginning with the launch of Nimbus 4 and after Nimbus 3 had been in orbit for one year .....	36
9	Illustration of a possible long period variation in the solar irradiance observed with sensor A from Nimbus 3 and 4. The enhancement represents the departure from an exponential degradation of the 30-day averages of signal which have been corrected for the changing sun-earth distance. Sensors B, C did not show this enhancement .....	37
10	Flare associated enhancement of uv irradiance observed from Nimbus 3 at the end of the first week in orbit. The term $f(\theta)/\cos \theta$ is a normalization function to correct for changing angles of solar illumination .....	38

# SPACE OBSERVATIONS OF THE VARIABILITY OF SOLAR IRRADIANCE IN THE NEAR AND FAR ULTRAVIOLET

## INTRODUCTION

An experiment designated MUSE (Monitor of Ultraviolet Solar Energy) was designed to measure the solar irradiance in the 1100-3000Å region with high photometric accuracy in bands of several hundred Angstroms width over long periods from space. The principal goal of the experiment was to determine the magnitude and time scale of possible variations in the solar irradiance which provides the principal radiative input into the lower thermosphere, mesosphere, and upper stratosphere. Variations of solar uv flux have been mentioned in the past in an attempt to explain apparent correlations between certain indices of solar activity and amounts of trace constituents which are in photochemical equilibrium, the temperature structure of the atmosphere, and the question of the variability of the solar constant. Various reported time scales for the solar and related atmospheric phenomena, apart from diurnal and seasonal effects, cover a wide range, i.e. from minutes to hours for solar flares, to a 27-day period associated with solar rotation; a 26-month quasi-biennial variation in atmospheric temperature, total ozone, and tropopause height but with no observed solar activity with this period; and the 11-year sunspot cycle. Solar radiation in the 1100-3000Å region is also of interest to solar physics since it covers the transition region from photospheric to chromospheric radiation which is a consequence of the increasing opacity of the solar atmosphere with decreasing wavelength.



The period of the solar observations reported here extends from August 1966 (near solar minimum) through March 1972 (past solar maximum) during which period the MUSE experiment has been flown three times. A model of the Nimbus satellite instrument was flown to an altitude of 210 km on board an inertially stabilized Aerobee 150 in August 1966. Subsequently a common set of three sensors was on Nimbus 3, launched on April 14, 1969, and on Nimbus 4, launched on April 8, 1970. The Nimbus 4 experiment is still operational while the one on Nimbus 3 worked up to January 22, 1972 when the Nimbus 3 operations were terminated. The orbits of Nimbus 3 and 4 are circular, sun-synchronous, and polar at a nominal altitude of 1100 km. The ascending mode of the orbits cross the equator near local noon.

Another experiment on Nimbus 4 provided some complementary measurements of the solar irradiance at 12 discrete wavelengths in the range from 2550 to 3400Å. The latter experiment, designated BUV (Backscatter Ultra-violet) used a double monochromator designed for the primary purpose of measuring the terrestrial uv albedo on a global basis, to be used for the determination of the global distribution of atmospheric ozone. However, the present paper is concerned only with the secondary objective of this BUV experiment, i.e. to obtain occasional data on the solar irradiance incident on the terrestrial atmosphere from observations possible only near the northern terminator transits.

The series of solar observations from August 1966 through the present (March 1972) has provided evidence for four types of variability in the solar irradiance from 1100-3000Å. In order of increasing period they are: flare enhancements, observed only with the sensor sensitive to H Lyman alpha; a

27 day variability corresponding to the solar rotational period which has come predominantly from two active regions about  $180^\circ$  apart in solar longitude; two maxima about 23 months apart, observed only in H Lyman alpha; and a long-term variability observed over at least half of the 11-year solar cycle, with an apparent maximum effect near 1800A.

## INSTRUMENT

The sensor system of the MUSE experiment consists of five vacuum photodiodes which were fabricated by the EMR Photoelectric Division of Weston Instruments, Inc. The photodiodes have a nominal  $90^\circ$  field of view, and they are mounted between bays of the Nimbus sensory ring in the direction of  $180^\circ$  from the spacecraft velocity vector. In this location the sensors are fully illuminated by the sun for about 20 minutes of each 107 min. orbit. The sensors are illuminated at near normal incidence when crossing the terminator in the northern polar regions. The angle of solar illumination of the sensors at the terminator for Nimbus 3 was within the range of  $0-20^\circ$  from the time of launch through the termination of spacecraft operations. On Nimbus 4, this angle of illumination has been within the limits of  $-3^\circ$  to  $+7^\circ$ . The angle of solar illumination relative to the normal of the face of a sensor is measured with a resolution of  $0.70^\circ$  by a solar aspect sensor (made by Adcole Corp.).

The wavelength selectivity of a sensor is produced by using a suitable radiation resistant optical filter (Heath and Sacher, 1966) to provide the short wavelength cut-off while the long wavelength rejection is achieved through the use of photocathode materials of varying degrees of "solar blindness". The sensor response function (filter transmittance x quantum efficiency) for the

three sensors common to the three flights are given in Figure 1. Sensor A has a  $\text{MgF}_2$  window in front of an opaque tungsten photocathode. Both sensors B and C have an outer  $\text{Al}_2\text{O}_3$  radiation shield which has a vacuum deposited metallic grid for electrical shielding. The response of B is determined by fused  $\text{SiO}_2$  filter in front of a semi-transparent  $\text{CuI}$  photocathode which was deposited on a  $\text{Al}_2\text{O}_3$  window. Similarly a combination of fused  $\text{SiO}_2$  with an aluminum neutral density coating and  $\text{CaCO}_3$  (calcite) in front of a semi-transparent photocathode of  $\text{CsTe}$  on  $\text{Al}_2\text{O}_3$  was used for sensor C.

The photodiode currents are amplified by an electrometer with automatic range-switching over four decades. The dynamic range extends from a minimum discernible current of  $5 \times 10^{-13}$  amp on Nimbus 3 and  $2.5 \times 10^{-13}$  amp on Nimbus 4 to  $1 \times 10^{-7}$  amp for full scale on the least sensitive range. The typical photodiode dark current is  $1 \times 10^{-14}$  amperes. The linear electrometer is automatically zeroed once every program cycle of 48 seconds. An in-flight calibration of the electrometer is made by sequentially sampling constant-current sources every 48 seconds. The constant-current sources which consist of ionization chambers excited by Americium 241 foils are not affected by temperature variations or by the high energy particle space environment. The long-term stability of the constant-current sources and of the electrometer of Nimbus 3 are illustrated in Table 1. This same degree of stability is also typical of Nimbus 4.

The output current from each of the five photodiodes is sequentially switched by reed relays into a common electrometer for 5 seconds of each cycle of 48 seconds. The sampling period of the electrometer output is 1.0 second for Nimbus 3 and 0.5 seconds for Nimbus 4. The remaining 23 seconds

of an experiment cycle are used for synchronization, for automatic nulling of the electrometer, and for the electrometer calibration with the constant current sources.

Measurements of the solar irradiance at 12 discrete wavelengths from 2550-3400Å with a 10Å band pass are being made with a tandem Ebert-Fastie type double monochromator on Nimbus 4 (BUV experiment). In the latter experiment the monochromator views a solar illuminated diffuser plate. Therefore the solar irradiance can be measured only at the northern terminator. This double monochromator will be described in detail in a paper to be submitted to "Applied Optics" at a later date.

#### RADIOMETRIC CALIBRATION

The basis for directly comparing the uv solar flux measured from the rocket in 1966 and that from the Nimbus satellites 3 and 4 in 1969 and 1970 respectively has been a standard vacuum photodiode which consists of a semi-transparent CsTe photocathode on a  $\text{Al}_2\text{O}_3$  window.

In 1966 this diode was calibrated at 2537Å against an Eppley Thermopile which, in turn, had been calibrated against a standard of total irradiance. The calibration of the diode at 2537Å was transferred onto a photomultiplier equipped with a freshly deposited film of sodium salicylate in front of its window. Another calibration point was obtained at 1216Å using a previously calibrated NO cell. Assuming the response of the sodium salicylate film to be constant over this wavelength range, we found that the two end points of this preliminary calibration agreed within 15%. This preliminary calibration was then used for the standard CsTe diode over the wavelength range of

1450-2500Å. The calibration at wavelengths beyond 2500Å was made using interference filters. The output of the diode was compared directly with the output of the thermopile when viewing the radiation from a high intensity source transmitted by the interference filters.

In late 1970 the aforementioned standard photodiode was recalibrated from 1450-2300Å by the group under Dr. Madden at the National Bureau of Standards in terms of a standard of total irradiance. A similar calibration at wavelengths beyond 2500Å was made by Optronic Laboratories. The agreement between the calibration at 2537Å made in early 1966 to that made in late 1970 by independent means was better than 5%. The 1970 calibrations were used to correct the preliminary calibration of the standard detector made in 1966. All values given in this paper reflect the 1970 calibration. A combination of the standard diode and a photomultiplier was calibrated for the 1050-1600Å region by the sodium salicylate technique, using to the quantum efficiency of the standard diode as a reference for the 1450-1600Å region. The long term stability and effects of the high energy particle environment for the type of photodiodes used in the MUSE experiment have been discussed previously (Heath and McElaney, 1968). The relative intensity distribution of solar radiation within the spectral bandpass of the detector was assumed to be known to an accuracy better than that of the absolute quantum efficiency of the detector. The absolute spectroradiometric calibration of the MUSE sensor B is considered accurate to about 15%. Sensor A because of its low sensitivity and short wavelength response, and sensor C, because of the need to use a neutral density filter to reduce the sensor current, are probably calibrated to an accuracy of no better than 20%.

The BUV instrument (to be described in detail elsewhere) was calibrated with a 1000 watt tungsten quartz iodine lamp used as a standard of spectral irradiance. The uncertainty in standard is 8% at 2500A, 4% at 2900A and 3% for the region of interest beyond 3000A. The basic limitation on the accuracy of the measurements of solar irradiance contained in Table 3 is the accuracy of the standard of spectral irradiance.

## OBSERVATIONS

### Absolute UV Solar Irradiance and the Solar Cycle.

The technique of making photometric measurements of irradiance with broad-band detectors is capable of high photometric accuracy since one can use vacuum photodiodes and filters which are relatively unaffected by signal/noise, small variations in the applied operating voltage, angle of illumination, and temperature. A fundamental limitation of this technique is presented by the need to rely on other knowledge of the actual solar spectral intensity distribution within the passband of the detector. The following sources for measurements of solar irradiance were used in predicting the MUSE sensor outputs:

- 1) 1027-1775A (Hinteregger, et al., 1964)
- 2) 1800-2600A (Detwiler, et al., 1961)
- 3) 2600-4000A (Tousey, 1963)

The sensor response at a given wavelength,  $\lambda$ , is given as the sum from 0 to  $\lambda$  of the product of the filter transmission, photocathode quantum efficiency, and the solar irradiance. These functions are shown in Figure 2 for

the three sensors A, B, and C which were used in the three flights of the MUSE experiment, and D and E which were only on Nimbus 4. The labeling of the curves corresponds to that used in Table 2. The curves which correspond to the rocket flight and flights of Nimbus 3 and 4 are designated R, 3 and 4 respectively. Values of the solar irradiance which are listed for column (a) of Table 2 were used to calculate the curves 3'A, 3C, 4C, RC, 4D, and 4E as shown in Figure 2. The tabulation of solar irradiance listed in column (b) of Table 2 was used to produce the curves 3A, 4A, and RA. The response function curves 3B, 4B, and RB were calculated using equivalent blackbody solar disc temperatures of 4700, 4650, and 4500 K respectively for the solar irradiance.

A comparison of the predicted sensor outputs with those actually observed is given in Table 2. The ratios of the predicted signals to those observed are listed under column (a) for the three sensors which were common to the three flights. The ratios for two additional sensors which used interference filters (2220A, 2820A) but were flown only on Nimbus 4, are also listed.

The 1966 rocket flight carried two sensors other than those listed in Table 2. One used an  $\text{Al}_2\text{O}_3$  filter in conjunction with a CuI photocathode to give a median sensor response at 1740A with 50% of the signal originating within a 155A band. The ratio of the calculated to the observed signal was 6.1. The other sensor used a CsI photocathode in conjunction with an ADP filter which produced a signal lower than expected.

The Nimbus 3 experiment also had two sensors besides those listed in Table 2. The additional short-wavelength sensor used a CuI photocathode deposited on a  $\text{CaF}_2$  window and it had a gridded  $\text{MgF}_2$  window for electrical

shielding. Unfortunately the Nimbus 3 satellite was launched into a major geomagnetic storm. This, combined with the solar uv, produced a signal degradation of about 25% per orbit in this channel for the early orbits. Extrapolation of the degradation back to orbit 1 gives a calculated to observed signal ratio of 2.8 under the conditions listed for column (2) of Table 2. Fifty percent of the signal came from a 170A band centered at 1750A. The other sensor excluded from the list of Table 2 used an ADP filter in conjunction with a CsI photocathode. Its exclusion is due to some serious problems encountered with this type of sensor. A discussion of these problems, however, is not within the scope of the present paper.

The measurements of the solar irradiance which were made by the BUV experiment on Nimbus 4 are given in Table 3. The double monochromator had a spectral band pass of 10A and a triangular slit function. A comparison of these Nimbus measurements with a revision of the NRL data by Thekaekara (1970), that of Labs and Neckel (1968, 1970), Makarova and Kharitonov (1969), and Tousey (1963) is shown in Figure 3. In this figure the values of solar irradiance are integrated over 100A intervals except for the measurements with the BUV experiment and the values listed by Labs and Neckels (1968) beyond 3275A. The best overall agreement in the range of 2550-3400A appears to be with the compilation by Makarova and Kharitonov (1969). Below 3000A there is good agreement with the NRL rocket data (Tousey, 1963) however, at longer wavelengths the NRL values of solar irradiance are considerably higher than those given here for Nimbus 4.



The observations with the double monochromator are consistent in general with the observations of sensor C of the MUSE experiment. Sensor C on Nimbus 4 indicates that the NRL published values of solar irradiance are only about 13% higher than that observed with sensor C whose median response is at 2870Å with 50% of the signal originating in the band from 2620-3030Å. It can be seen in Figure 3 that the BUV experiment indicates that the solar irradiance is within a few percent of the NRL values. Thus the MUSE and BUV experiments are consistent in their region of overlap.

Recently, new observations of the uv solar intensity have been reported for the period spanned by the MUSE observations. Rocketborne spectrophotometer observations of the solar spectrum between 1400 and 1815Å were made on September 24, 1968, and have been published by Parkinson and Reeves (1969). An analysis of ten solar rocket spectra obtained on July 27, 1966 has been published by Widing, Purcell, and Sandlin (1970). The first year of operation of the MUSE experiment is overlapped by observations of H Lyman alpha from OSO-4, which have been published by Timothy and Timothy (1970).

On July 11, 1968 an Air Force satellite, OVI-15, was launched and carried an Aerospace Corporation photodiode experiment for observations of the solar irradiance in the 300-2100Å region. Data from the Aerospace Corp. experiment were recorded for the 27 days of the satellite's lifetime, which have subsequently been published by Prag and Morse (1970).

A comparison of the equivalent blackbody solar temperatures observed by the NRL, Harvard, and Aerospace groups are shown for comparison in Table 4. The effective temperatures were estimated on the basis of a background

effective temperature of 4440K and an estimated calcium plage contribution, and were provided by a referee. In 1966 it is seen readily that the MUSE rocket observations of solar irradiance are significantly lower (about a factor of three) than the NRL values for a rocket flight about a month earlier. The difference cannot be due to atmospheric attenuation since the MUSE experiment reached an apogee of 210 km. The solar attenuation at the peak of the Schumann-Runge continuum (1450A) at 200 km for a 60° solar zenith angle is only 2.3% for a Jacchia 1965 model atmosphere for  $T = 806\text{K}$  where  $n(\text{O}_2) = 3.49 \times 10^8 \text{ cm}^{-3}$  and the absorption cross section,  $\sigma = 1.44 \times 10^{-17} \text{ cm}^2$  (Watanabe, et al., 1953). At 1750A the corresponding solar attenuation would be only 0.04%.

The MUSE observations are reasonably consistent with measurements reported by Parkinson and Reeves (1969); consequently a value of  $T = 4500\text{K}$  was used to estimate the solar continuum in the response region of sensor A in conjunction with the measured H Lyman alpha irradiance of  $3.6 \times 10^{11} \text{ quanta/cm}^2 \text{ sec}$ , and the emission line tabulation by Hinteregger, et al., 1964. The ratios of calculated to observed signals for these conditions are given in column (b) in Table 2 where the agreement is within the limits of the experimental accuracy.

It is concluded that there is a significant variation in the solar irradiance in the vicinity of 1750A which is just to the long wavelength side of the solar temperature minimum. Furthermore, this variation appears to follow the 11 year solar cycle. The MUSE observations tend to support values of the solar irradiance which are consistent with the Harvard observations and significantly lower than those reported by NRL for wavelengths below 1800A. At

the longer wavelengths, 2500-3200A, there is reasonable agreement with the NRL observations. In the region from 3200 to 3400A the solar irradiance observed with the BUV experiment is significantly lower than the NRL value as is shown in Figure 5. There is some evidence shown in Table 2, Sensor C, for a long term solar cycle variation which borders on the limits of experimental error.

#### Variability of UV Irradiance with Solar Rotation.

As of March 1972, the MUSE experiments on Nimbus 3 and 4 had observed the sun through 39 rotations. The variability in the uv irradiance which is associated with the 27 day rotational period is easily detected since the amount of sensor degradation even under the worst cases was small during a 27 day rotational period. In general it has been observed that the sensor degradation can be well described by a straight line in a plot of the logarithm of the sensor current versus time, or by a series of straight lines of decreasing slope with increasing time (Heath, 1972). The smallness of the sensor degradation in conjunction with an extremely large signal to noise ratio and with the well stabilized sun synchronous satellite made it possible to detect changes in the uv irradiance of about 1% per solar rotation.

Figure 4 shows the corrected currents of the three sensors, A, B, and C for the terminator passages during the first year of operation of Nimbus 3. The sensor currents shown were corrected for degradation (exponential decay factor removed) so that the curves show the 27-day variability in irradiance essentially free of instrumental effects. Other indicators of solar activity are shown in the lower part of the figure. The 8-20A x-ray background flux data

which has had the flare enhancements subtracted out is from the Explorer 37 experiment of Kreplin of the Naval Research Laboratory. The values for the daily  $\Sigma Kp$  and the 10.7 cm solar flux are those listed in "Solar Geophysical Data" of the Environmental Data Service, NOAA.

Very significant variations in the uv solar irradiance do occur over a 27 day solar rotational period. In general, the maxima and minima in the uv irradiance coincide with those in the general indicators of solar activity, and the magnitude of the variation per solar rotation decreases as the wavelength of the sensor response increases. Figure 5 reveals a nearly linear relationship between the logarithm of the irradiance variation per solar rotation,  $(I_{\max} - I_{\min})/I_{\min}$  and the nominal photon energy, expressed by the wave number ( $\text{cm}^{-1}$ ) of the median response within the bandwidth of the sensor. The curve is for a particular solar rotation during the first six months of the operation of Nimbus 3. Qualitatively this relationship appears to be typical of all the observations with Nimbus 3 and 4. The three broad-band sensors are hardly sufficient to determine the true nature of the variation in the irradiance with wavelength. Therefore Figure 5 should be used only as a qualitative guide as to how the solar fluxes may vary in the spectral range spanned by the three sensors. Prag and Morse (1970) have reported on satellite observations of the solar irradiance from 300 to 2100A for 27 days of the satellites operation. In Figure 5 of their paper they present the signal changes observed from changes in the solar irradiance in the 300-1150A, 1150-1600A, and 1600-2100A regions between July 13 and August 9, 1968. Their data show an enhancement (as defined in the MUSE analysis) of about 2.6 for the two longer wavelength intervals. Since neither the sensors nor the time of observations were exactly alike it is

difficult to establish whether or not a contradiction exists between the two experiments. However similarities do exist between the two experiments. Their experiment was flown just prior to and the MUSE experiment just past solar maximum, and furthermore two of their sensors did overlap in response with the MUSE sensors A and B. Based on this and the size of the variations shown in Figure 4 of this paper the author feels that the magnitude of their reported variation of solar irradiance with rotation may be too large especially since data were reported for only one solar rotation.

The response of sensors A and B shown in Figure 4 reveals that one frequently observes two maxima in the irradiance per solar rotation. If the assumption is made that the maximum is observed when the active region is on the central meridian, then a graph of the Carrington longitude of the central meridian on the day of the uv irradiance maximum should indicate the longitude of the active regions. This is shown in Figure 6 for the period from April 1969 to March 1972. The accuracy in determining the uv maxima is about  $\pm 1$  day or  $\pm 13^\circ$ . Since April 1969 the MUSE experiment appears to have observed two active regions about  $180^\circ$  apart in longitude through 39 solar rotations. A third region almost midway between the two regions was detected in November 1970. Different symbols are used to identify the active regions on the basis of groupings in longitude in Figure 6.

The slope of the curves in Figure 6 may seem to indicate that the uv active regions do not have the same rotational periods as that assigned to the Carrington longitude system. The active region which was near a longitude of  $330^\circ$  in April 1969 has a synodic period of 27.45 days while the

one near a longitude of  $100^\circ$  at that time has a period of about 27.39 days. Obviously this difference is much less than the accuracy of  $\pm 1$  day in the identification of the observed uv maxima. The two long-lived active regions appear to have undergone some major change some time around April 1971, as is indicated by the broken lines in Figure 6.

The percentage variation in the uv irradiance per solar rotation is defined as  $100 (I_{\max} - I_{\min}) / I_{\min}$  where  $I_{\min}$  is the minimum value of the solar irradiance between two maxima.

The variations in the solar irradiance as observed with sensor A are given in Figure 7 for the period from April 1969 to March 1972. The symbols for the different active regions are consistent with those used in Figure 6. The two long-lived active regions which have been observed since the launch of Nimbus 3 suddenly increased to a level where the variation of the irradiance per rotation rose to about 50% above the background level between the solar rotations numbered 1547-1549. Since that time the variations have been oscillating but they appear to fall within an upper bound which is decreasing exponentially with time. The rate of decrease was about a factor of five over 25 revolutions of the sun. The error in the measurement of the change in the solar irradiance per rotation is about 1% which means that there is a possible 10% error in a measured 10% change in irradiance per solar rotation, and similarly a 20% error in an observed variation of 5%. Therefore, the oscillations within the exponential upper bound envelope should be considered as real. A comparison of a three-month overlap of the data from sensor A on Nimbus 3 and 4 is given in Figure 8. The Nimbus 4 curve most likely is more heavily

weighted towards H Lyman alpha, whereas the Nimbus 3 points probably reflect a large contribution from solar radiation in the 1400-1700A region. This statement reflects our judgement that after a year in space the radiation damage has reduced the response to 1216A more severely than that to longer wavelengths. This judgement is based on laboratory investigations.

The H Lyman alpha solar irradiance also has been measured at two day intervals since January 1969 by an experiment of Vidal-Madjar, Blamont, and Phissamay (1972) on OSO-5. For comparison purposes an attempt was made to determine the percentage variation per solar rotation,  $100 (I_{\max} - I_{\min}) / I_{\min}$  for the OSO-5 data for 1969 and 1970. The value for  $I_{\min}$  was determined from a linear interpolation between successive minima at 27 day intervals. If the four points where the MUSE-measured variations greater than 30% per solar rotation are excluded, a linear regression analysis yields a correlation coefficient of 0.71 between the two experiments and  $Y = 0.70X + 4.6$  where Y is the percentage variation measured from Nimbus 3 and 4 and X from OSO-5. These differences are probably due to the fact that the OSO-5 measurements reflect a 100A bandpass centered at Lyman alpha whereas the sensor A of the MUSE experiment is sensitive to Lyman alpha and the wider band from 1400-1700A which is shown in Figure 2.

The uv solar rotational variability has been compared to the conventional indicators of solar activity. Correlation coefficients were derived from a linear regression analysis of the percentage variation per solar rotation observed with sensor A and the 10.7 cm flux, the provisional mean Zurich sunspot numbers ( $R_z$ ), the calcium plage product of area and intensity, and the calcium

plage product of projected area and intensity. The results of this analysis for the period from April 1969 to July 1971 are given in Table 5. If all rotations are considered during this period, then  $R_z$  appears to be a better indicator of the solar uv activity; however, if solar rotations 1547-1549 for which the minimum between rotations was above the normal background level are excluded, then the Ca plage index is better.

#### A Possible 22 Month Solar Variability

From the assumed quasi-exponential decay of the instrumental sensitivity one would expect that a plot of the logarithm of the sensor current with time would consist of a series of straight lines of decreasing slope. Therefore some pronounced departures from this situation, observed with sensor A as shown in Figure 9, are noteworthy. The percentage enhancement of the 30 day signal averages above the expected signal decrease with time is shown for all times when it was greater than 3%. For the points shown in Figure 9 the uninteresting effect of the annual variation due to the change in the earth-sun distance has been removed. In the late spring of 1969 and early spring of 1971 the increase in the short wavelength solar irradiance was about five and two times greater than the annual variation, respectively.

Whether or not this observed solar uv enhancement has any connection with the well known biennial oscillation of the atmosphere is not known at present.

#### Flare-Related Variations of UV Irradiance.

A major solar flare of optical importance 3B, small class X which started at 19:59 U.T. on April 21, 1969 was observed at the end of the first week in



orbit of Nimbus 3, the MUSE observations of this event are shown in Figure 10. The ordinate is the sensor current normalized to the terminator value of orbit 101. To a first approximation the sensor response is proportional to the cosine of the angle of illumination. A small correction of the cosine response to changing angles of solar illumination is given by  $f(\theta)$  which is unique to each of the sensors. The normalized sensor A, B, C, signals are given for three orbits where the flare began 30 frames prior to the terminator crossing in orbit 102. Only the sensor for the shortest wavelengths showed any observable flare enhancement, greater than 1%. Unfortunately the data gap for orbit 102 is caused by not being able to record data during the satellite interrogation from the ground because of the failure of one of the on-board tape recorders. If an exponential decay for flare radiation is assumed then this would indicate an enhancement of 16% above the pre and post flare values of the solar radiation which produces the signal in channel A.

On the basis of measurements from OSO III Hall (1971) has published an empirical formula which relates the percentage enhancement of a line, E, from the total solar disc to the  $H_\alpha$ -flare area, A, expressed in heliocentric square degrees, e.g. for H Lyman alpha  $E = 0.3 A^{3/2}$ . Application of this formula to a flare observed with MUSE, i.e.  $A \doteq 15.3$  square degrees leads to a predicted enhancement of 18% which is in quite good agreement with the extrapolated value of 16% if it is assumed that the MUSE sensor responded principally to the flare in Lyman alpha.

## DISCUSSION

Results have been presented which have been obtained from a broad band photometer experiment flights on a rocket and the Nimbus 3 and 4 satellites along with spectrophotometer measurements from Nimbus 4 on the uv solar irradiance and variability in the 1100 to 3400A region. Large changes have been observed in the radiation originating in the chromosphere which are associated with solar flares, the 27 day solar rotational period and a possible biennial period. While the variations observed are largest at the shortest wavelengths, a rather large variation has been observed also in the wavelength band centered around 1750A. This variation appears to follow the eleven-year solar cycle. This large effect as observed with sensor B refers to radiation originating in the upper photosphere and the photosphere-chromosphere transition region. The latter is the region of the solar temperature minimum.

The variability in the uv solar irradiance which has been observed with the MUSE experiment over a portion of the 11 year solar cycle should be observable in the concentrations of trace constituents which are photochemical in origin. The most thoroughly documented case is that of ozone. An extensive review article on atmospheric ozone and solar ultraviolet radiation has been published by Dutsch (1969). In the region of photochemical equilibrium, up to the 1 mb level at least, the ozone concentration is proportional to the square root of the ratio of the number of dissociating quanta absorbed by one  $O_2$  molecule per second to the number of dissociating quanta absorbed by one  $O_3$  molecule per second. The variations from the mean of upper stratospheric ozone content (from 30 km to above 42.5 km) which are derived from the

Umkehr technique over Arosa are clearly shown by Dutsch (1969) over the period from 1956 to 1964. The magnitude of the variation increases with increasing altitude which implies that the variation in the solar uv should increase as the wavelength decreases, as was indeed observed with the MUSE experiment.

Variations in the vertical profile of atmospheric ozone above 20 km also have been reported by Paetzold (1969, 1971) from many flights of a balloon borne optical sonde over the period from 1951 to 1970. A very significant correlation was observed for both the ozone amount between 20 and 30 km and the amount of the ozone maximum with the sunspot Wolf numbers.

Further evidence corroborating the MUSE observations of long term changes in the uv solar irradiance may be found in the work of Gattinger and Jones (1966). They observed a four fold decrease in brightness of the 0, 1 band of the  $O_2$ ,  $^1\Delta_g - ^3\Sigma_g^-$  system over the years between 1960 and 1964. One of the theories for the production of  $O_2$  ( $^1\Delta_g$ ) invokes the dissociation of  $O_3$  in the Hartley continuum where the production rate of  $O_2$  ( $^1\Delta_g$ ) is proportional to the concentration of  $O_3$  and the number of dissociating quanta absorbed by one ozone molecule per second.

#### ACKNOWLEDGEMENTS

The very significant contributions of Mr. Raymond Westcott as technical officer of the MUSE experiment on Nimbus B, 3 and 4 are gratefully acknowledged as being a major factor in providing two spacecraft experiments, one of which operated until the Nimbus 3 operation was terminated deactivated and the other one which is still operating (Nimbus 4).

## REFERENCES

- Bumba, V., Large-scale magnetic field and activity patterns on the sun, Leningrad Symposium, IUCSTP, May 1970 (in press).
- Detwiler, C. R., Garrett, D. L. Purcell, J. D., and Tousey, R., The intensity distribution in the ultraviolet solar spectrum, *Ann. Geophys.*, 17, 263, 1961.
- Dodson, H. W., Comments on large scale organization of solar activity in time and space, *AIAA Bulletin*, 7, 563, 1970 (Abstract).
- Dutsch, H. U., Atmospheric ozone and ultraviolet radiation, *World Survey of Climatology*, Vol. 4, *Climate of the Free Atmosphere*, Elsevier Publishing Co., 383, 1969.
- Eddy, J. A., Lena, P. J., and MacQueen, R. M., Far infrared measurement of the solar minimum temperature, *Solar Physics* 10, 330, 1969.
- Gattinger, R. L. and Jones, A. V., The  $^1\Delta_g - ^3\Sigma_g^+$ ,  $O_2$  bands in the twilight and day airglow, *Planet. Space Sci.*, 14, 1, 1966.
- Hall, L. A., Solar flares in the extreme ultraviolet, *Solar Physics*, 21, 167, 1971.
- Heath, D. F. and Sacher, P. A., Effects of a simulated high-energy space environment on the ultraviolet transmittance of optical materials between 1050 and 3000A, *Appl. Opt.*, 5, 937, 1966.
- Heath, D. F. and McElaney, J. H., Effects of a high-energy particle environment on the quantum efficiency of spectrally selective photocathodes for the middle and vacuum ultraviolet, *Appl. Opt.*, 7, 2049, 1968.

- Heath, D. F., Observations on degradation of uv systems on Nimbus spacecraft, International Commission for Optics, IX, Oct. 9-13, 1972, Santa Monica, Ca. (to be published in proceedings.)
- Hinteregger, H. E., Hall, L. A., and Schmidtke, G., Solar XUV radiation and neutral particle distribution in July 1963 thermosphere, Space Research V, Amsterdam, North Holland Publ. Co., 1175, 1964.
- Hudson, R. D., Carter, V. L., and Breig, E. L., Predissociation in the Schumann-Range Band system of O<sub>2</sub>: Laboratory Measurements and Atmospheric effects, J. Geophys., Res., 74, 4079, 1969.
- Labs, D. and Neckel, H., The radiation of the solar photosphere from 2000A to 100 $\mu$  Z. Astrophys., 69, 1, 1968.
- Labs, D. and Neckel, H., Transformation of the absolute solar radiation data into the 'International Practical Temperature Scale of 1968,' Solar Phys., 15, 79, 1970.
- Makarova, E. A. and Kharitonov, A. V., Mean absolute energy distribution in the solar spectrum from 1800A to 4mm, and the solar constant, Soviet Astronomy A.J., 12, 599, 1969.
- Paetzold, H. K., The photochemistry of the atmospheric ozone layer, Symposium on Chemical Reactions in the Lower and Upper Atmosphere, Stanford, 1961.
- Paetzold, H. K., Variation of the vertical ozone profile over middle Europe from 1951 to 1968, Am. Geophys., 25, 347, 1969.

- Paetzold, H. K., Secular variations of the atmospheric ozone layer over middle Europe from 1951 to 1968, XV General Assembly, I.U.G.G., Moscow, 1971.
- Parkinson, W. H. and Reeves, E. M., Measurements in the solar spectrum between 1400 and 1875A with a rocket-borne spectrometer, *Solar Phys.* 10, 342, 1969.
- Prag, A. B. and Morse, F. A., Variations in the solar ultraviolet flux from July 13 to August 9, 1968, *J. Geophys. Res.*, 75, 4613 (1970).
- Thekaekara, M. P., Proposed standard values of the solar constant and the solar spectrum, *J. Environmental Sc.*, 13, 1970.
- Timothy, A. F. and Timothy, J. G., Long-term intensity variations in the solar helium II Lyman alpha line, *J. Geophys. Res.*, 6950, 1970.
- Tousey, R., The extreme ultraviolet spectrum of the sun, *Space Sci. Rev.*, 2, 1, 1963.
- Vidal-Madjar, A., Blamont, J. E., and Phissamay, B., Solar Lyman alpha changes and related hydrogen density distribution at the earth's exobase (1969-1970), COSPAR XV, Madrid, Spain, 1972.
- Watanabe, K., Inn, E. C. Y., and Zelikoff, M., Absorption coefficients of oxygen in the vacuum ultraviolet, *J. Chem. Phys.* 21, 1026, 1953.
- Widing, K. G., Purcell, J. D. and Sandlin, G. D., The uv continuum 1450-2100A and the problem of the solar temperature minimum, *Solar Phys.*, 12, 52, 1970.

Table 1

Stability of the Constant Current Calibration Sources Measured  
with the MUSE Electrometer on Nimbus 3 (Nominal 5000 Orbits/yr.)

Orbit No.:	Thermal Vac	2	800	4000	12476
Source No.	Current (amperes)				
1	3.74E(-11)	3.73E(-11)	3.94E(-11)	3.91E(-11)	3.84E(-11)
2	2.85E(-10)	2.81E(-10)	2.99E(-10)	2.98E(-10)	2.96E(-10)
3	5.64E(-10)	5.57E(-10)	5.91E(-10)	5.90E(-10)	5.86E(-10)
4	1.95E(-9)	1.92E(-9)	1.97E(-9)	1.98E(-9)	2.00E(-9)
5	9.53E(-9)	1.28E(-8)	1.04E(-8)	1.05E(-8)	1.05E(-8)

Table 2

## Ratio of Calculated to Observed Signals

	A		B		D	E	C
LAUNCH, YEAR	a	b	a	c	a	a	a
AEROBEE, 1966	1.26	1.13	4.83	4485			1.26
		(1216A)	(1770)				(2940A)
NIMBUS 3, 1969	1.61	1.09	1.98	4715K			0.83
	(1470A)	(1216A)	(1770A)				(2930A)
NIMBUS 4, 1970	0.94	0.83	2.60	4635K	1.09	0.83	0.87
		(1216A)	(1740)		(2220A)	(2820A)	(2870A)

a Signals calculated using the fluxes tabulated by Hinteregger, et al., 1964, Detwiler, et al., 1961 and Tousey, 1963.

b Signals calculated using H Ly  $\alpha$  flux of Timothy and Timothy (1970), other emission lines from Hinteregger, et al., 1964, and solar continuum at 4500 K.

c Equivalent blackbody temperature of solar disc to give solar irradiance observed with sensor B.

The wavelength of the median of the sensor response is in brackets.



Table 3

Solar Irradiance Measured with a 10A Bandpass and Triangular Slit Function

Vacuum Wavelength (A)	Irradiance (ergs/cm <sup>2</sup> -sec-A)
2557.0	10.7
2736.8	23.5
2830.7	39.1
2876.7	39.0
2922.6	63.8
2976.2	61.9
3020.3	49.0
3059.0	63.2
3125.9	71.0
3176.2	82.3
3312.9	94.6
3399.4	97.2

Table 4

## Equivalent Solar Blackbody Temperatures

Wavelength (A)	Temperature (K)	Date	Source
1750	4750 <sup>1</sup>	7-27-66	NRL, rocket
1770	4485 <sup>2</sup>	8-29-66	MUSE, rocket
1750	4590 <sup>2, e</sup>	8-29-66	Aerospace (extrapolation) OVI-15
1750	4600 <sup>1</sup>	10-24-68	Harvard, rocket
1770	4715 <sup>2</sup>	4-15-69	MUSE, Nimbus 3
1750	4660 <sup>2, e</sup>	4-15-69	Aerospace (extrapolation) OVI-15
1740	4635 <sup>2</sup>	4-8-70	MUSE, Nimbus 4
	4691 <sup>2</sup>	4-20-70	Aerospace (extrapolation) OVI-15

<sup>1</sup>Effective blackbody temperature of solar continuum at center of disc

<sup>2</sup>Effective blackbody temperature of observed solar irradiance

<sup>e</sup>Extrapolation of measurements of Prag and Morse (1970) which are based on background effective temperature of 4440K and estimated calcium plage contribution on indicated date (supplied by referee)

Table 5

Correlation Coefficients of UV Solar Irradiance Maxima from Sensor A with  
the Maxima of some Conventional Indicators of Solar Activity

	10.7	$R_z$	Ca Plage (AI)	Ca Plage ( $A_{proj}$ I)
All maxima	0.38	0.59	0.55	0.51
Solar rotations				
1547-1549 excluded	0.51	0.52	0.66	0.65

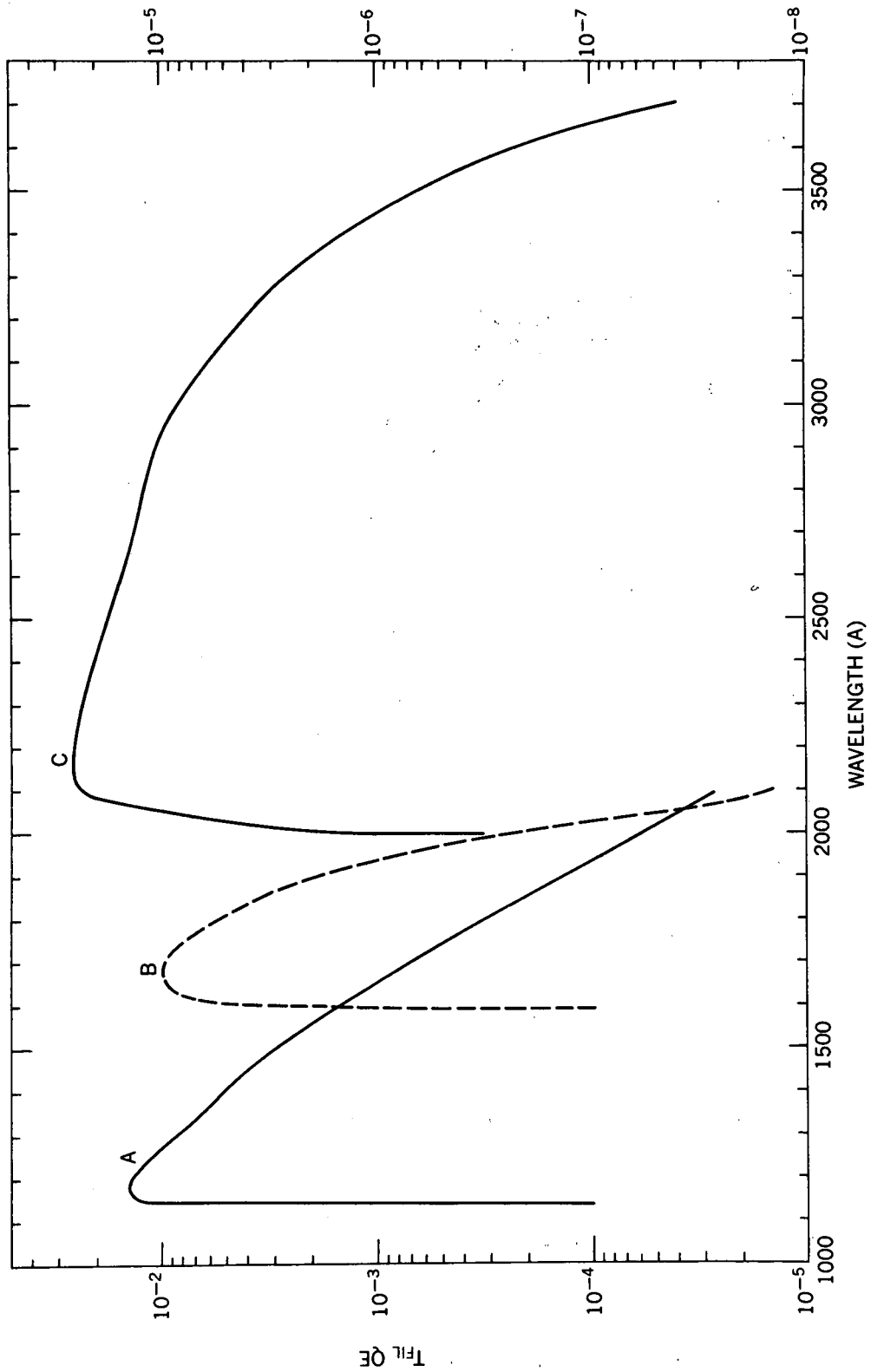


Figure 1. Product of filter transmittance and photocathode quantum efficiency. The left ordinate is for sensors A and B while the right one is for C.

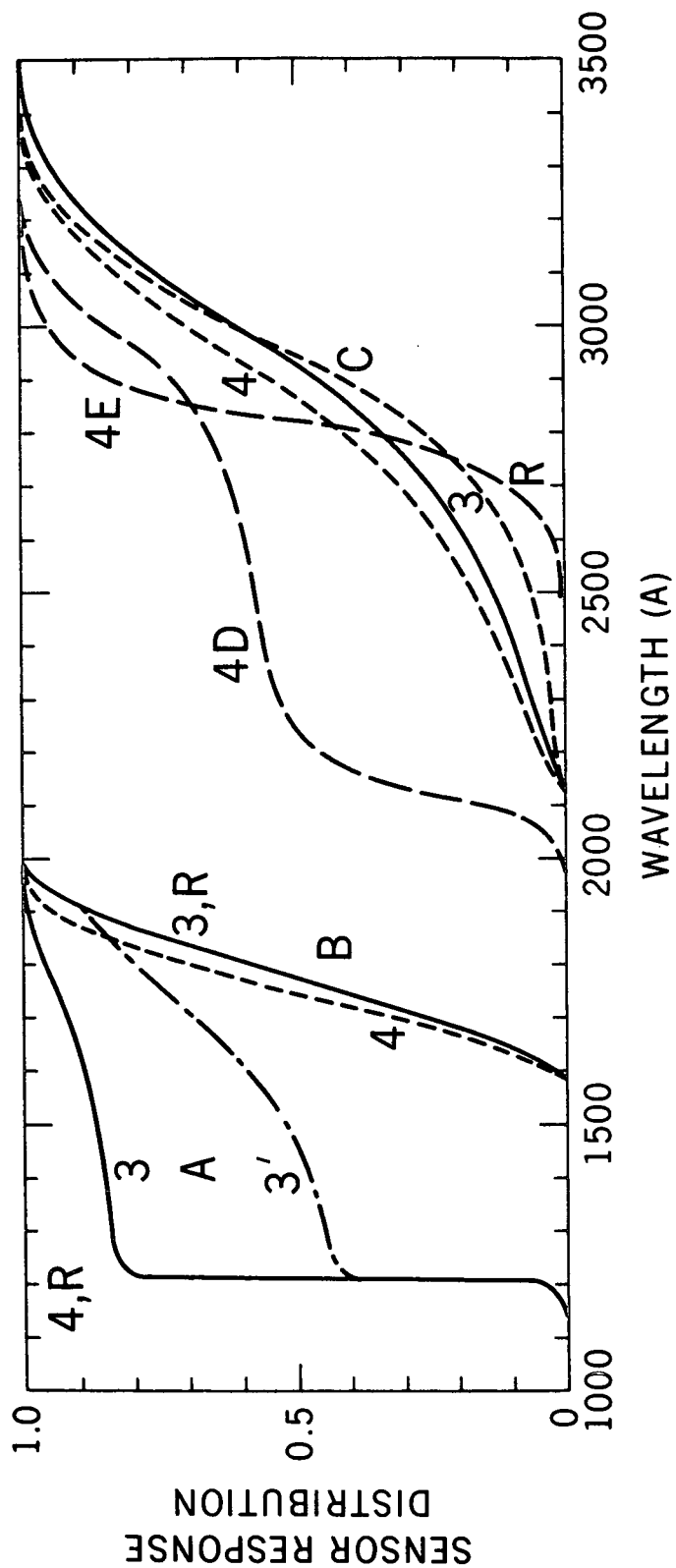


Figure 2. Sensor response distribution is the fractional part of the total signal coming from wavelengths less than . The letters A-E refer to the sensors listed in Table 2. The sensitivity curves (product of filter transmittance and photocathode quantum efficiency for sensors A-C) are shown in Figure 1.

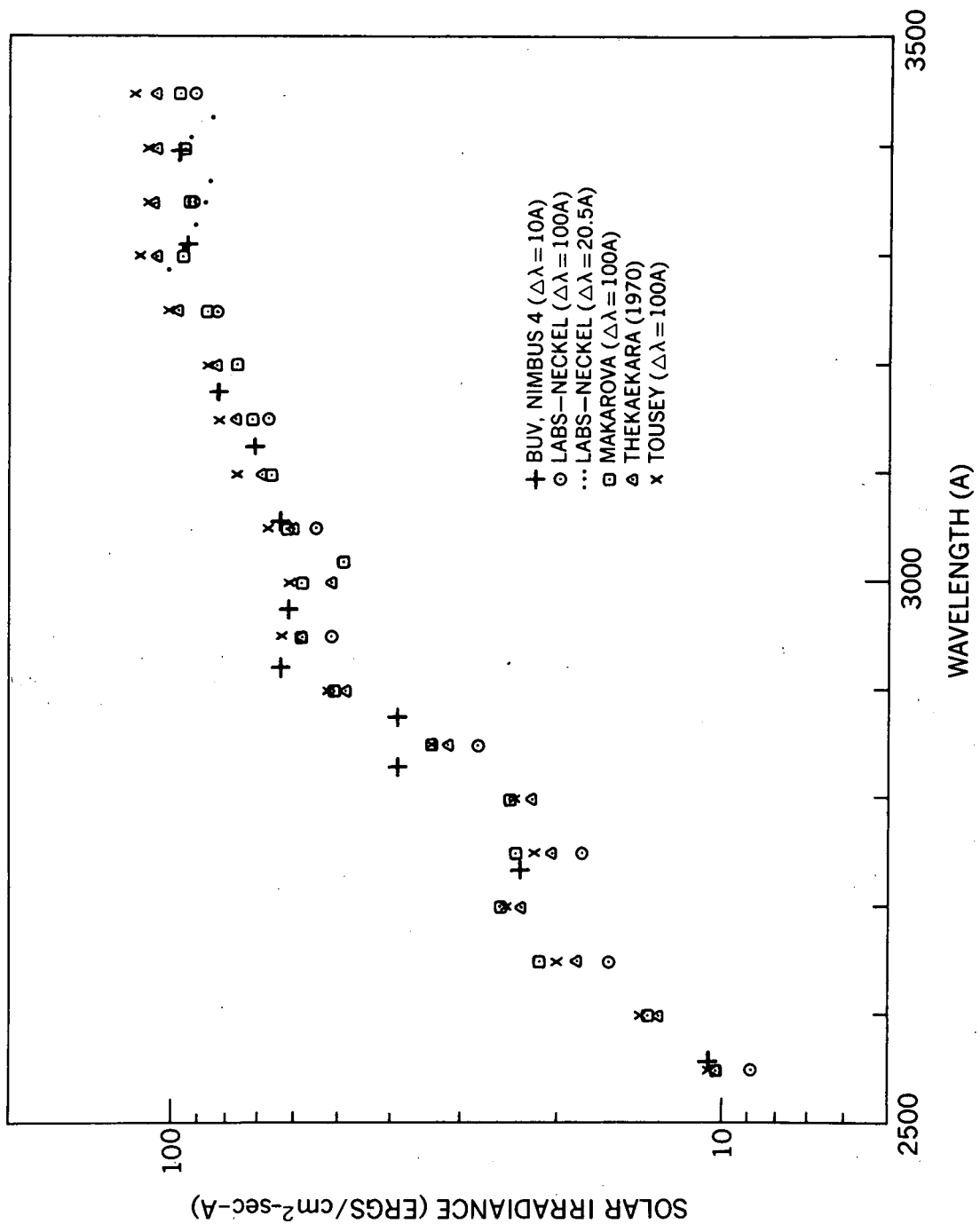


Figure 3. Comparison of solar irradiance observed from Nimbus 4 with the Thekaekara (1970), Labs and Neckel (1968, 1970), Makarova and Kharitonov (1969), and Tousey (1963).

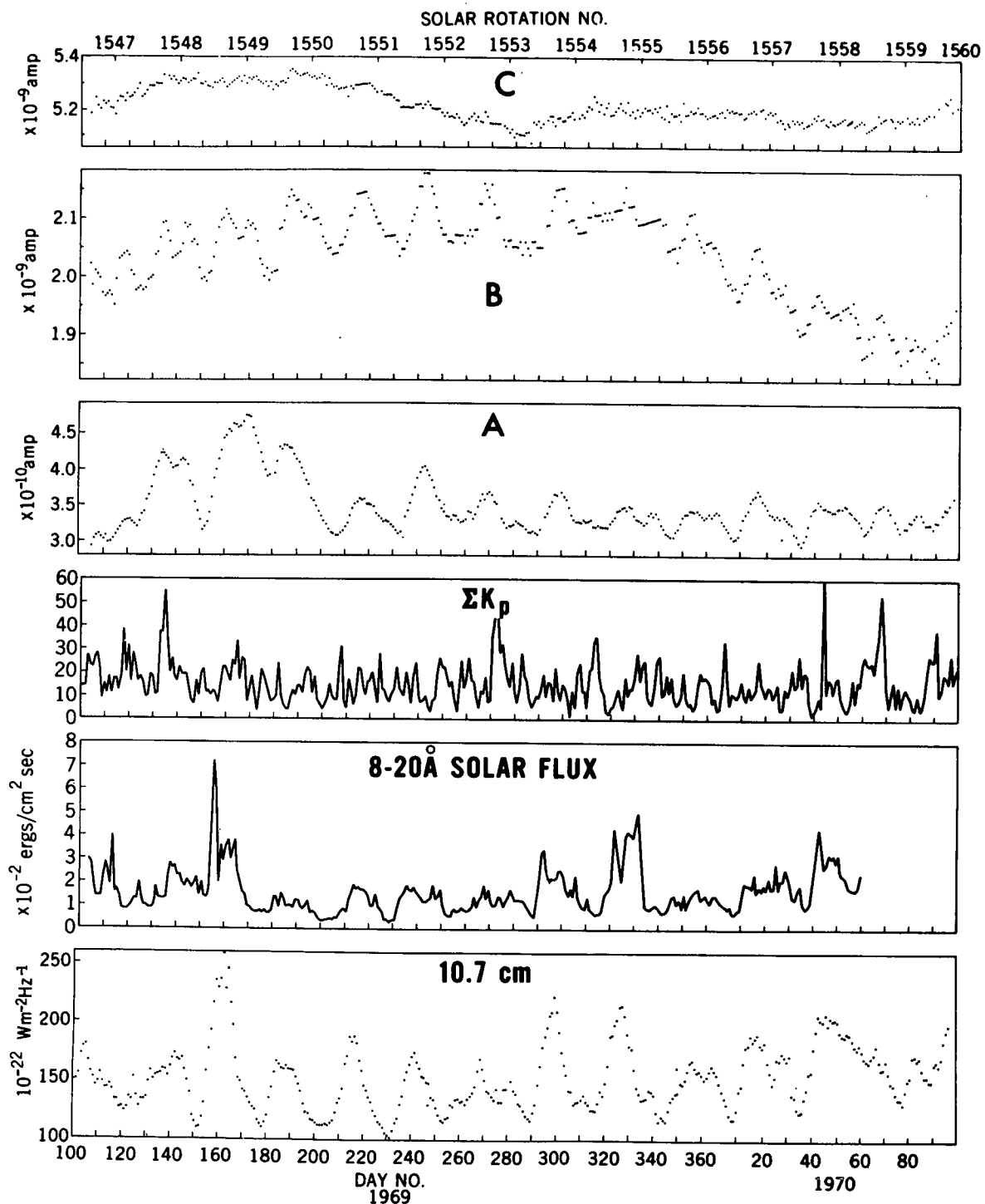


Figure 4. The MUSE sensor signal currents with the exponential degradation factors removed are given to illustrate the nature of variations in irradiance associated with the 27-day solar rotational period. Other indicators of solar activity are given for the same period.

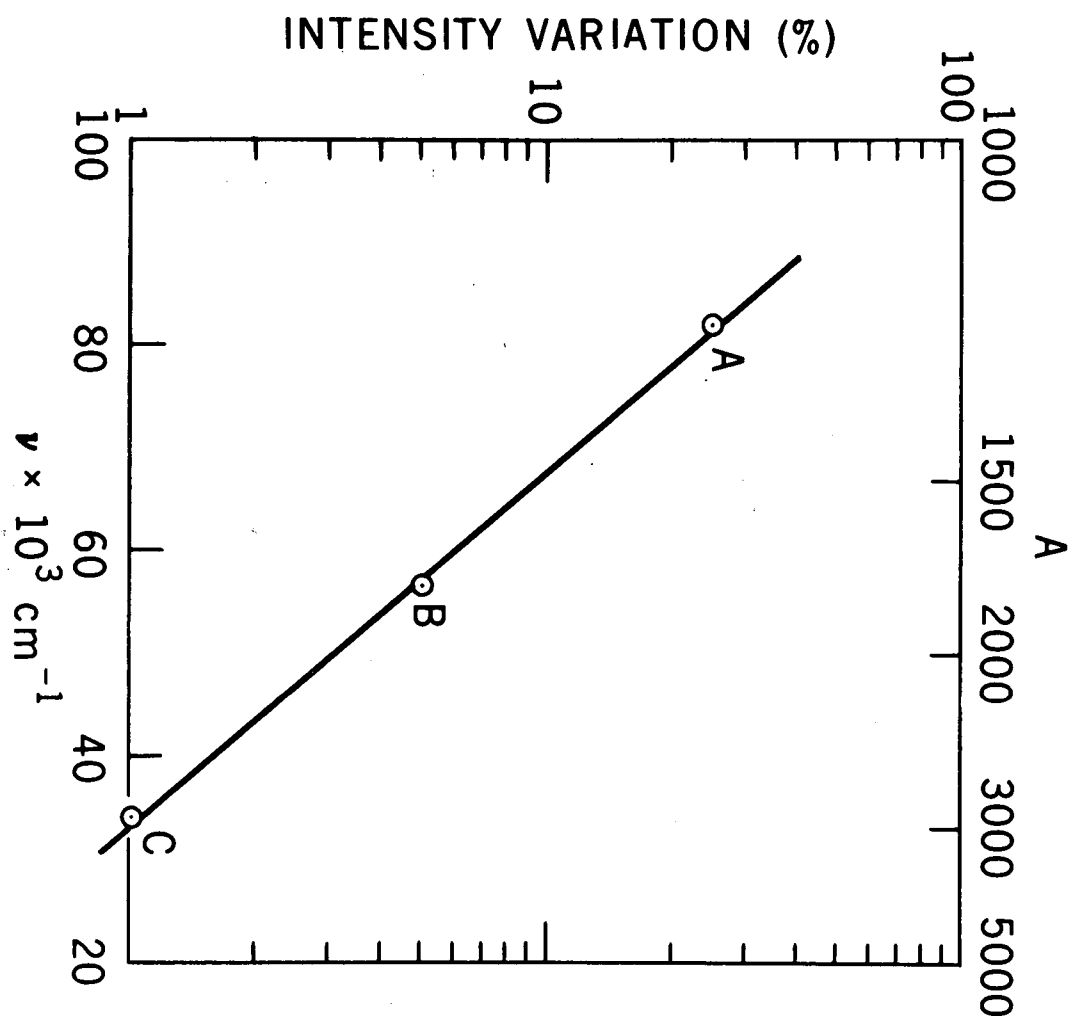
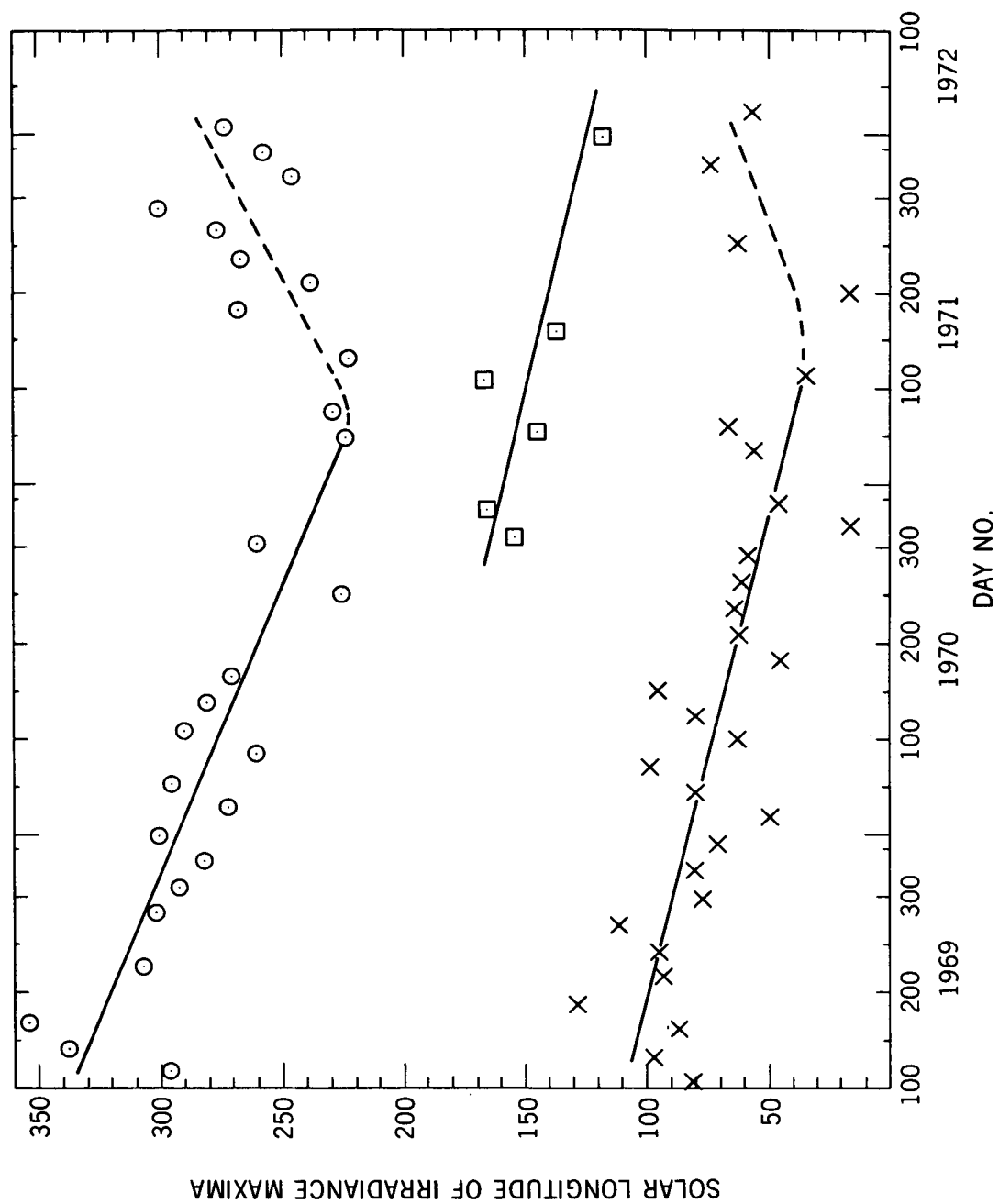


Figure 5. Percentage uv variation per solar rotation ( $I_{\text{max}} - I_{\text{min}} / I_{\text{min}}$ ) with the wavenumber of the 0.5 point in Figure 2 observed with the three sensors on Nimbus 3 near solar maximum.





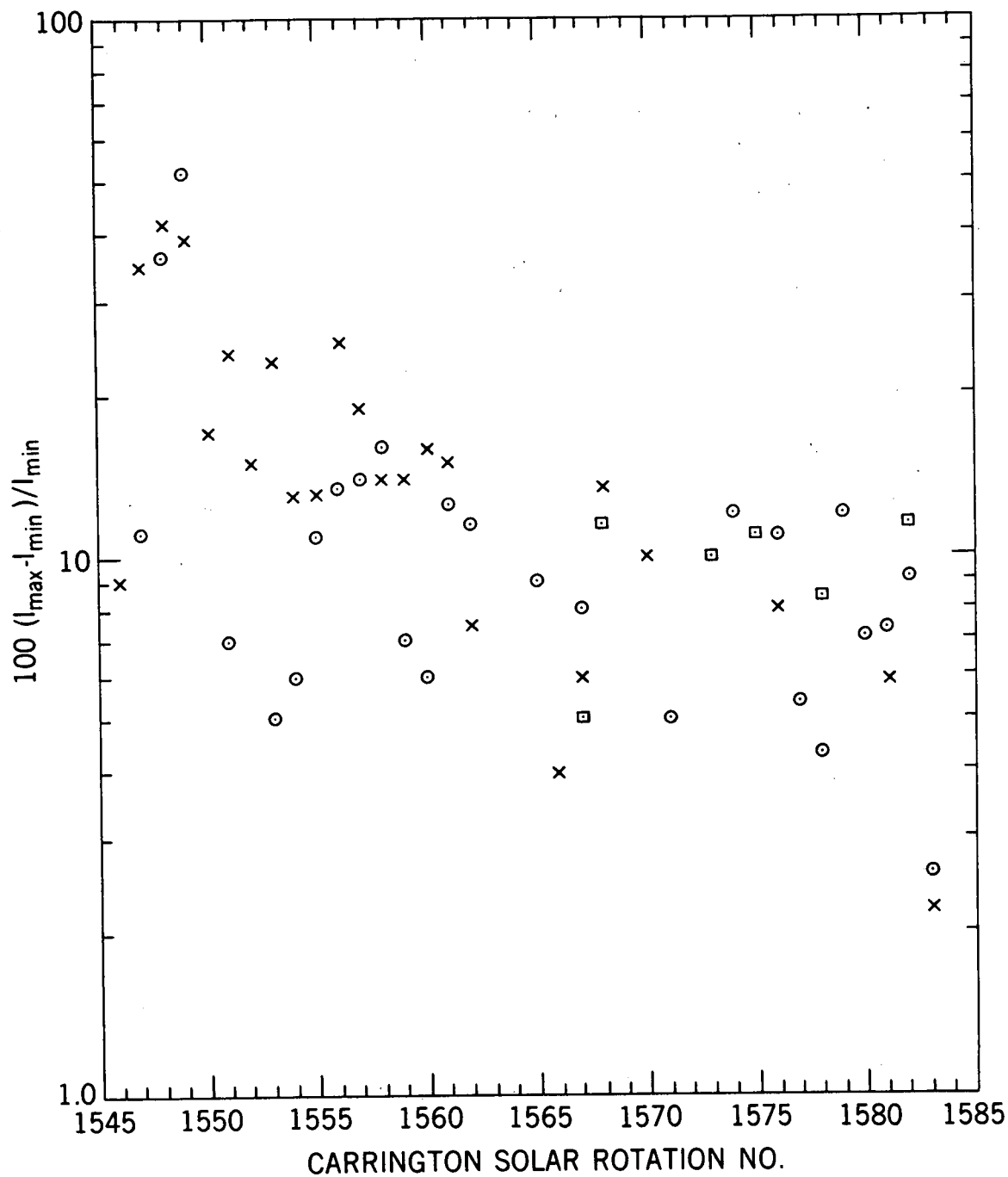


Figure 7. Observations of the percentage variation per solar rotation observed with sensor A on Nimbus 3 and 4.

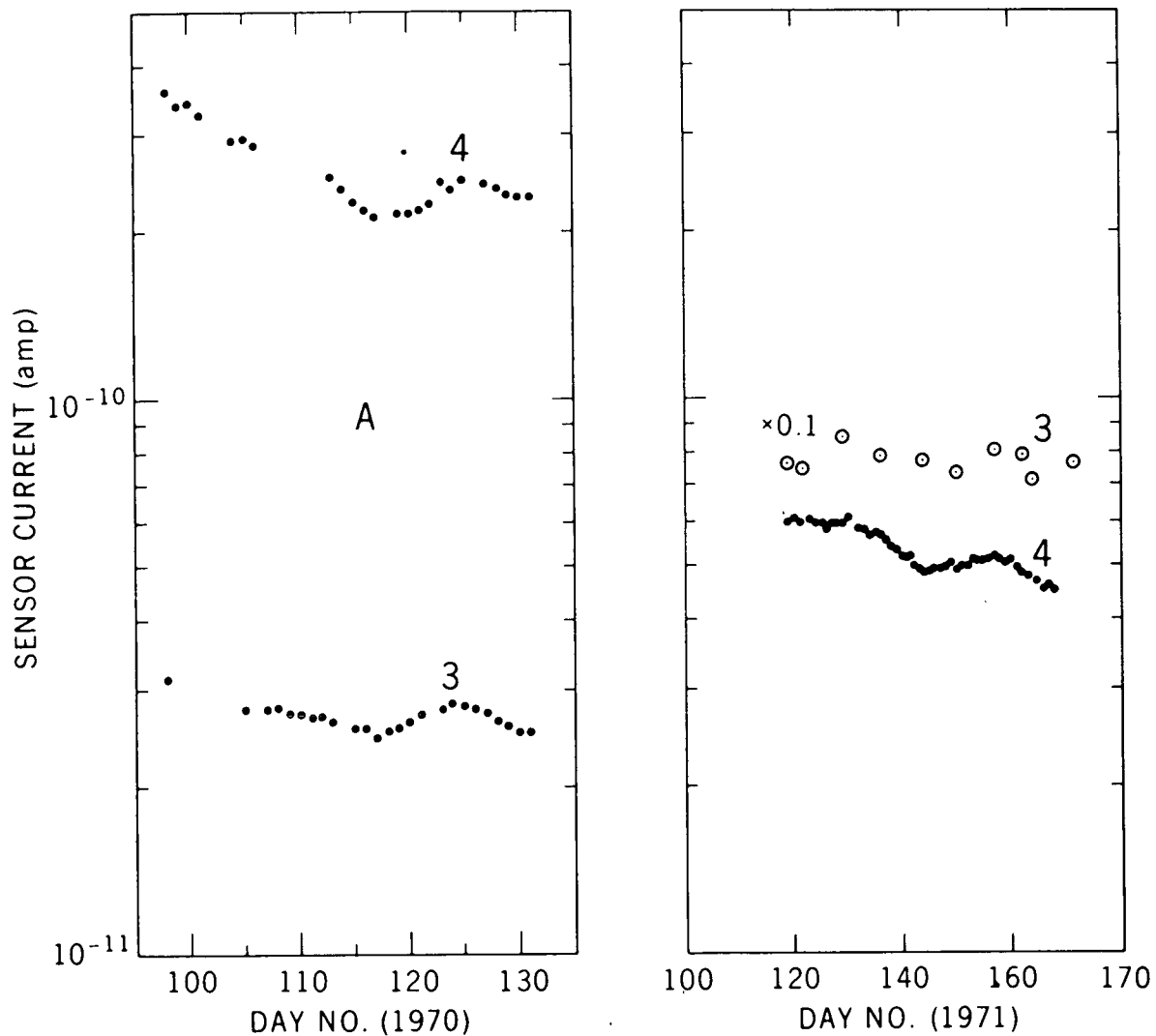
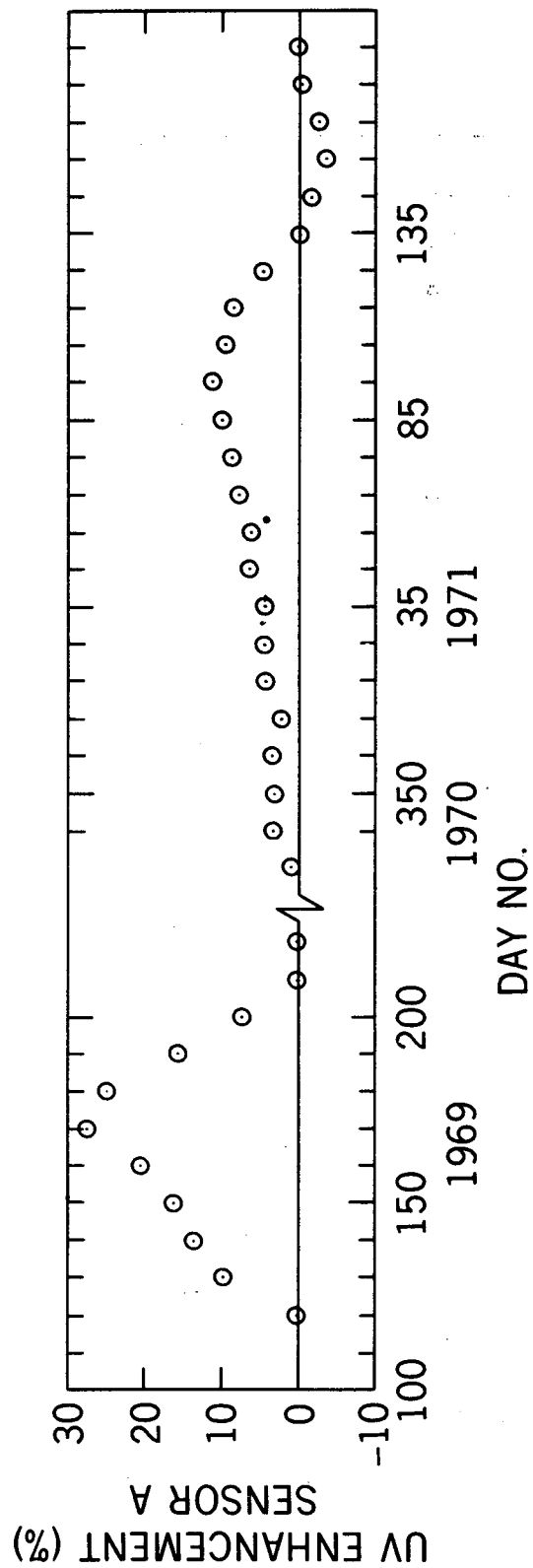


Figure 8. Overlap in time of the sensor A signals observed from Nimbus 3 and 4 for the period beginning with the launch of Nimbus 4 and after Nimbus 3 had been in orbit for one year.



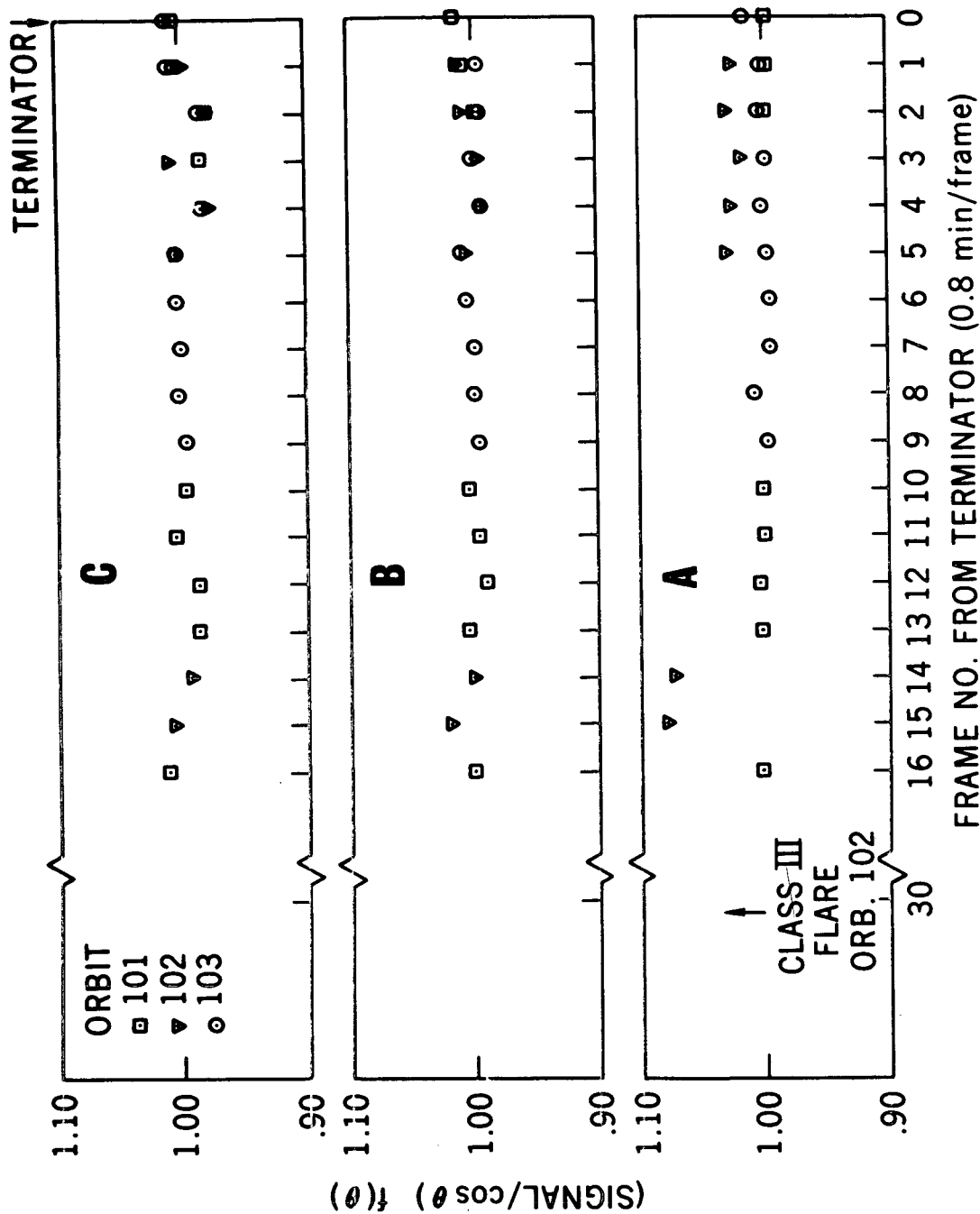


Figure 10. Flare associated enhancement of uv irradiance observed from Nimbus 3 at the end of the first week in orbit. The term  $f(\theta)/\cos \theta$  is a normalization function to correct for changing angles of solar illumination.